

CONTEXTUALITY OF QUANTUM STATES: THEORETICAL ANALYSIS AND EXPERIMENTAL INVESTIGATIONS



A thesis submitted towards partial fulfilment of
BS-MS Dual Degree Programme

by

MANVENDRA SHARMA

under the guidance of

DR. T.S. MAHESH

ASSISTANT PROFESSOR

INDIAN INSTITUTE OF SCIENCE EDUCATION AND RESEARCH
PUNE

Certificate

This is to certify that this thesis entitled "Contextuality of quantum states: Theoretical Analysis and Experimental Investigations" submitted towards the partial fulfillment of the BS-MS dual degree programme at the Indian Institute of Science Education and Research, Pune represents original research carried out by "Manvendra Sharma " at "Indian Institute Of Science Education And Research, Pune", under the supervision of "Dr T. S. Mahesh" during the academic year 2011-2012.

Student
MANVENDRA
SHARMA

Supervisor
DR T.S. MAHESH

Acknowledgements

I express my deepest gratitude to my supervisor Dr. T. S. Mahesh for his guidance, advice and moral support. I am very thankful to Dr. Mahesh for introducing me to the field of NMR. For last three years he has been a constant source of inspiration and motivation in my life. I would like to thank Professor Apoorva Patel of IISc Bangalore for his valuable time. Discussions with him on the basic problems of quantum physics were very helpful for me in understanding the subject and completing this thesis. I thank all faculties of IISER Pune for the valuable course work given by them in my masters.

I would like to thank my labmates Soumya Singha Roy, Abhishek Shukla, Swati Hegde, and Hemant Katiyar for debates on different concepts. I owe my humble gratitude to Soumya Singha Roy and Abhishek Shukla for helping me in experiments and motivating me throughout. I convey my special thanks to Sheetal Jain for his consistent and continuous support. I am indebted to my friends Anuj More, Ashwin Vyas, Vivekananda Reddy, Dinesh Kumar, and Akshat Yadav for encouraging me throughout this final year. I want to convey my hearty thanks to my batchmates for being with me all the time when I needed them in these five years of my life. Words cannot express my gratitude to my family for their blessings and support without which it would not have been possible to complete this thesis. In the end I would like to convey my thank to Lord Krishna for everything.

Abstract

It is a common notion in classical mechanics that the result of a measurement depends on the observable measured and the system in consideration. From the measurement outcomes, it is possible to assign the pre-measurement state of the system. But the same may not hold in quantum mechanics. Quantum mechanics is known to be a contextual theory. We cannot assign the pre-measurement states from the measurement outcomes, and hence quantum states can be contextual. We have done theoretical analysis and experimental demonstration of quantum contextuality. I have studied Bell's inequality and Kochen- Specker theorem. There are many forms of quantum contextuality. We have demonstrated Peres contextuality experimentally. We have taken a two spin half system to do the experiment. We have used a newly discovered technique in NMR called Moussa protocol. The results are in good accordance with the theory. We are also reporting continuously varying contextual operators. Inequality for spin 1 particle is also studied, which is called the pentagram inequality. Fully contextual quantum correlations were also studied.

Contents

1	Introduction	4
1.1	The History	4
1.1.1	An Important Point to Make	5
1.2	Literature survey	5
2	Theory	6
2.1	Bell's Inequalities	7
2.1.1	Bell's Theorem	8
2.2	Contextuality	9
2.2.1	Context of Measurement	9
2.2.2	Functional Consistency of a Measurement	10
2.2.3	Kochen-Specker Theorem	10
2.3	Peres Contextuality	11
2.3.1	Extension of Peres Contextuality	11
2.4	Spin 1 Case	13
2.5	Fully Contextual Correlations	13
3	Methods	15
3.1	NMR Implementation	15
3.1.1	Projective Measurement	17
3.1.2	Density Matrix Tomography	17
3.1.3	Singlet Preparation	18
3.2	Experiments	20
4	Results	23
4.1	Continuous Operator for Demonstration of Contextuality	23
4.2	Preparation of High Quality Singlet State	23
4.3	Obtaining Contextual Expectation Values	23
5	Discussion	26

References	27
A Long Proofs	30
A.1 Calculation of Left Hand Side of Equation 2.5	30

Chapter 1

Introduction

In their historical paper Einstein, Podolsky, and Rosen (EPR) claimed that Quantum theory is not complete[1]. Since then people started the everlasting search of cases which can ensure that quantum theory is a special kind of theory and it does not need to fulfill the requirements of classical world. Soon after this people started to find cases which can show that Quantum theory is not intuitive to human mind. John Bell got the first success in these attempts. In his pioneering paper he was the first to show that local hidden variable theories cannot predict the outcomes of Quantum Mechanics[1].

In statistical classical mechanics we can predict some parameters for the system. Although we don't know these parameters for individual atoms but can predict the statistical behavior of the system. The parameters for individual atoms can be considered as hidden variables, although we don't measure them directly but taking statistical average over them gives us the accurate result for the system in consideration. Initially, same was thought for quantum theory as well, but eventually it became clear that the same is not true for quantum mechanics. For the measurements outcomes of certain quantum systems one cannot pre-assign the numerical values for the results obtained. This property is known as quantum contextuality. Non-contextual hidden variable theories cannot predict the outcomes for quantum mechanics for any type of hidden variable.

1.1 The History

Kochen-Specker first showed that if the statistical results of quantum mechanics are to be reproduced while assuming the pre-assignment of the measurable outcomes, then that theory has to be contextual[4]. Peres in 1990 showed contextuality for singlet state of two spin $1/2$ particles in a single page

paper[2]. Mermin's four dimension case was state independent[13]. Klyachko *et al.* in 2008 showed a Bell like inequality for spin 1 particles. They called it pentagram inequality[17]. Cabello has recently showed that any state independent contextualitiy can be converted into an inequality which will be followed by local hidden variable theories but will be violated by Quantum mechanics[6]. Now, there are many versions of contextualities available.

1.1.1 An Important Point to Make

We have demonstrated the first experiment to verify Peres contextuality through NMR. In 2010, Moussa *et al.* demonstrated the Mermin's contextuality for four dimensions through NMR and gave the new technique emulated Moussa Protocol. We have used the same technique to do our experiment. Peres contextuality is given only for a single point. We have reported a new case in which the contextual operators are varied continuously. Details about the new case can be found in Sec. 2.3.1.

1.2 Literature survey

Controversy about quantum mechanics began with EPR paper in which they asked the question "Is quantum mechanics complete?" Bohr gave a reply to them in his paper[1]. But the first established reply was given by Bell in 1964 by giving the Bell inequalities[3]. Bell's argument was based on many experiments. So, after Bell, Kochen and Specker gave a theorem which proved that quantum mechanics cannot be described by non-contextual hidden variable theories[4]. Then physicists gave many arrangements of operators which resulted in the contradiction if the value of measurement is pre-assigned. Peres and Mermin gave the contextuality for state dependent case[2][13][14]. If we consider singlet state then we can prove contextuality for that particular system. But now there are state independent contextuality as well. Cabello has shown a similar case for two spin half qubits. Kochen Specker Theorem requires at least 31 rays (operators) for proof in three dimensions but Alexander A. Klyachko *et al.* have given pentagram inequality which we can test experimentally with only 5 rays (operators)[17]. But this pentagram inequality is state dependent. Experiment for pentagram inequality is also done for the LASER[18].

Chapter 2

Theory

The Quantum Physics faces some strong opposition since its birth; However none of the arguments stands tall against it for long. Many physicists including Einstein were not comfortable with the formulation of Quantum Mechanics (QM) in which evolution of a system is deterministic, but measurement outcomes are probabilistic and argues that quantum mechanics is rather an incomplete theory. These riddles have perplexed physicists ever since the formulation of quantum theory. In an attempt to make quantum mechanics more 'complete', many physicists tried to explain it by some classical models with hidden variables. Since then it has been a constant source of debate-whether hidden variables theories are compatible with Quantum theories or not. In a seminal paper in 1935, Einstein, Rosen, and Podolsky proposed an example which seriously questioned about the foundation of quantum mechanics, famously known as EPR paradox[1]. Consider a simple system having two particles A and B in a singlet state separated by a large distance (so that no instantaneous interaction between them is possible). Now, if an observer measures the angular momentum of A about any axis, the angular momentum of B about the same axis is instantaneously known (a paradox) and has same magnitude with opposite direction. The EPR paradox was unanswered until 1964, when John Bell showed that certain types of classical models cannot explain the quantum mechanical predictions for specific states of distant particles. Bell's Theorem proved that quantum mechanical expectation values cannot be represented by local-hidden variable theories and he gave a famous inequality later known as Bell's Inequality (BI)[3]. As was the case of hidden variable theories which were hard to test experimentally, BI was certainly less harder to test experimentally. These experimental tests widely used to test local hidden variable theories based on the assumption of 'locality'. The maximum entangled states (subsequently known as Bell's states) showed violation of BI and hence disproof the hidden variable theories

in general. The quantum physics, as we know of it today, seems to defy one of the 'Locality' (an event is independent of parameters controlled by other at distant spatial agents at the same time) or 'Realism' (system is in a certain state, the measurement just reveals that state) if taken at the same time. A more generalized form of hidden variables theorem came subsequently given by Bell, Kochen, and Specker. The Bell-Kochen-Specker showed that certain types of hidden variables cannot render quantum mechanics as a deterministic theory. Recently, the Bell-Kochen-Specker Theorem has been extensively tested experimentally with various experimental quantum mechanical setup such as nuclear spins, neutrons, photons, trapped ions etc[7, 8, 9, 10, 11].

2.1 Bell's Inequalities

Bell in 1964 showed in his paper that quantum mechanics is incompatible with the Einstein locality. He showed that in any theory there will be an upper limit on the correlations of distant events, if one assumes principle of local cause. But the correlations in quantum mechanics were found to be above that upper limit. To check this let us assume an experiment of exploding bomb. Let the angular momentum of the two parts be J_1 and J_2 , where $J_1 = -J_2$. Now an observer measures the dynamical variable $(\alpha \cdot J_1)$, where α is a unit vector in an arbitrary direction chosen by the observer. The result of this measurement is called 'a' which can take only value ± 1 . Similarly for a second observer who measures the dynamical variable $(\beta \cdot J_2)$, where β is chosen by the second observer. The measurement result of second observer is called 'b'. b can only take value ± 1 . If the experiment is repeated N times and a_j and b_j are the results obtained by observers for the j^{th} case, the average would be $\langle a \rangle = \sum_j a_j / N$ and $\langle b \rangle = \sum_j b_j / N$, but the correlation between the results of the observers will be $\langle ab \rangle = \sum_j a_j b_j / N$ which, in general, does not vanish. For example, if we take $\alpha = \beta$, then we will always get $a_j = -b_j$. In that case $\langle ab \rangle = -1$. For arbitrary α and β , to calculate the expected correlation $\langle ab \rangle$, we can consider a unit sphere. To decide the value of a , imagine an equatorial plane perpendicular to α , which divide the sphere into two hemispheres as in Figure 2.2. Observer can then decide that $a = 1$ if J_1 points through one of the hemispheres and $a = -1$ in other case. A similar equatorial plane can be drawn to decide $b = \pm 1$. These two equatorial planes divide the sphere into four sectors. Adjacent sectors have their areas in the ratio θ to $\pi - \theta$, where θ is angle between α and β . We have assumed uniform distribution of J_1 . So the classical correlation will be $\langle ab \rangle = [\theta - (\pi - \theta)] / \pi = -1 + 2\theta / \pi$.

For quantum mechanics, we can take two spin 1/2 particles in a sin-

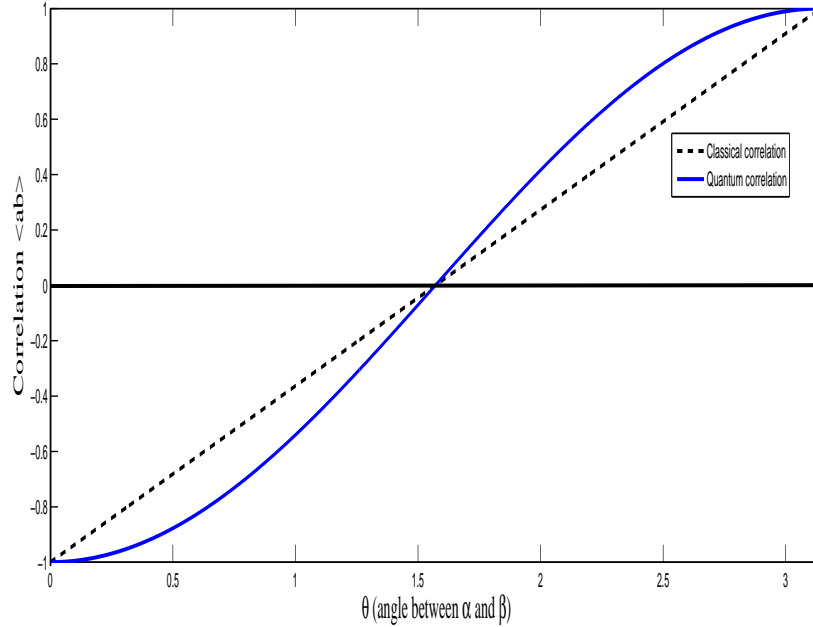


Figure 2.1: The solid line shows the quantum correlations, the dotted line shows classical correlations

glet state, far away from each other. In this case, observers measure the observables $\alpha \cdot \sigma_1$ and $\beta \cdot \sigma_2$, where σ_1 and σ_2 are the Pauli spin matrices. The unit vectors α and β are arbitrary selected. The results a and b can have values ± 1 . Their mean values as predicted by quantum mechanics will be $\langle a \rangle = \langle b \rangle = 0$, and their quantum correlation will be $\langle ab \rangle = \psi^\dagger (\alpha \cdot \sigma_1) (\beta \cdot \sigma_2) \psi$. For a singlet state, we know $\sigma_2 \psi = -\sigma_1 \psi$. Using the identity $(\alpha \cdot \sigma_1) (\beta \cdot \sigma_2) \equiv \alpha \cdot \beta + i(\alpha \times \beta) \cdot \sigma$, we can get the quantum correlations $\langle ab \rangle = -\alpha \cdot \beta = \cos \theta$. Thus, we can say classical and quantum mechanical correlations are quite different. It can be seen from the graph that the quantum correlations are stronger than the classical one except for the values of $\theta \in \{0, \pi/2, \pi\}$ [16].

2.1.1 Bell's Theorem

Now lets consider a pair of polarized photons emitted in opposite directions. Let the observers measure the linear polarization of these photons. First observer has choice of making the orientation of his polarizer in two different directions having angle α and γ with respect to some arbitrary axis. If the axis with the orientation α is chosen then the outcome is called 'a' and for γ it

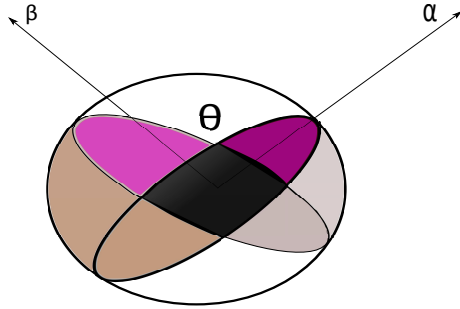


Figure 2.2: The Sphere for classical correlations

is called 'c'. 'a' and 'c' can only take values ± 1 . The other observer has choice of choosing the directions β and γ , giving the corresponding results as 'b' and 'c' respectively. Same as a and c , b also can take only value ± 1 . The equality $a(b-c) \equiv \pm(1-bc)$ always holds for any combination of allowed (± 1) values of a , b , and c . If the same experiment is repeated several times, the j^{th} photon pair will satisfy $a_j b_j - a_j c_j \equiv \pm(1 - b_j c_j)$. Now, taking the average over j , we get $|\langle ab \rangle - \langle ac \rangle| \leq 1 - \langle bc \rangle$. $\langle ab \rangle$ is the correlation of the outcomes a and b . The above result is known as Bell's Inequality. For the polarized photons, the above expression becomes $|\cos 2(\alpha - \beta) - \cos 2(\alpha - \gamma)| + \cos 2(\beta - \gamma) \leq 1$. For example: if we take the angles between α , β and γ to be 30° , then the above inequality will be violated. Polarized photons violate the Bell's Inequality[16].

2.2 Contextuality

As we have seen in the previous section that the violation of the Bell's inequality occurs only at statistical levels, it is hard to observe it experimentally. Every such experiment would be a suspect of non ideal quantum detector. Contextuality is a counterfactual paradox which does not depend on any particular state and therefore can be tested without becoming victim of problems posed due to statistical inferences.

2.2.1 Context of Measurement

Let us consider an operator A . If A commutes with some other operators B and C , then one can measure A along with B or along with C . The result of measurement of A will not differ when A is measured along with B or C . It means measurement of A is context independent. Here we are considering both the cases: (1) When B and C are measured on different

physical systems, (2) When B and C are measured for the same system as A . For example, we can take A as the square of the angular momentum (J^2) of a particle. Now J^2 commutes with the angular momentum components J_x and J_y of the same particle (B and C). But J_x does not commute with J_y . We can say that measurement of J^2 yields the same value in all the cases: performed alone, together with J_x and J_y , one of the two. But we cannot test it experimentally in a single experiment, as J_x and J_y does not commute. So they cannot be measured simultaneously.

2.2.2 Functional Consistency of a Measurement

If two operators (A and B) mutually commute then we can say that that we can measure them and any function of them ($f(A, B)$) simultaneously. If a system is prepared in state ψ such that $A\psi = \alpha\psi$ and $B\psi = \beta\psi$, then we can assume $f(A, B)\psi = f(\alpha, \beta)\psi$. This means that the eigenvalues will have the same functional relationship as the eigenvectors.

Now if we take both context and functional consistency of a measurement, then they are incompatible with quantum mechanics. For example, we can take the following square array of operators for a pair of spin 1/2 particles. In the array all the operators in a row or column commute among themselves

$\mathbb{1} \otimes \sigma_z$	$\sigma_z \otimes \mathbb{1}$	$\sigma_z \otimes \sigma_z$	$+\mathbb{1}$
$\sigma_x \otimes \mathbb{1}$	$\mathbb{1} \otimes \sigma_x$	$\sigma_x \otimes \sigma_x$	$+\mathbb{1}$
$\sigma_x \otimes \sigma_z$	$\sigma_z \otimes \sigma_x$	$\sigma_y \otimes \sigma_y$	$+\mathbb{1}$
$+\mathbb{1}$	$+\mathbb{1}$	$-\mathbb{1}$	

and have eigenvalues ± 1 . For each row and column the third operator is the product of other two, but in the third column we have to put a minus sign to get the operator. So if we assume that measurement is context free and holds functional consistency, then we will always end up with some contradiction for the above array. In other words, there is no way to assign ± 1 values to the measurement outcomes of each of these 3×3 operators which satisfy the results of the combined measurements in each row and each column[16].

2.2.3 Kochen-Specker Theorem

According to Kochen-Specker Theorem, for a Hilbert space of dimension ≥ 3 , it is not possible to assign numerical values $\nu(p_m)$ (such that $\sum \nu(p_m) = 1$) for each member of a complete set of commuting projection operators, P_m . The first proof of K-S theorem included 117 rays, but after that the minimum number of rays required for 3 dimensional case were thought of being 31.

Recently a proof with only 13 rays has also been reported[12]. But proof for 4 dimensional case can be given by 11 rays only [16].

2.3 Peres Contextuality

In 1990, Asher Peres described a simple situation where the following intuitive assumptions contradict the quantum theory: (I) the result of the measurement of an operator depends only on the operator being measured and the state of the system, and (II) if operators A and B commute, the result of a measurement of their product AB is the product of the results of separate measurements of A and B . In the following paragraph, we attempt to explain Peres contextuality [2]. Consider a system of two spin 1/2 particles in singlet state $(|01\rangle - |10\rangle)/\sqrt{2}$, Here $|0\rangle$ and $|1\rangle$ are eigen states of σ_z . The result of a single measurement of σ_x^1 , the component of the first spin along x direction can be either $+1$ or -1 , the eigenvalues of σ_x^1 . The non contextual theories try to assign one of these values just before the actual measurement takes place. According to the non contextual theories, the measurement just reveals the pre-assigned value. Let the assigned value for σ_x^1 measurement be x_1 . Similarly, σ_y^1 measurement be y_1 , σ_z^1 measurement be z_1 and so on. The result of measuring $\sigma_x^1\sigma_x^2$ must be -1 because, $\langle\sigma_x^1\sigma_x^2\rangle = -1$ for the singlet state. Similarly, we have $\langle\sigma_y^1\sigma_y^2\rangle = -1$ and $\langle\sigma_z^1\sigma_z^2\rangle = -1$ for the singlet state. From the assumption II, it follows that

$$x_1x_2 = -1, y_1y_2 = -1, z_1z_2 = -1. \quad (2.1)$$

Since $[\sigma_x^1\sigma_y^2, \sigma_y^1\sigma_x^2] = 0$, the operators $\sigma_x^1\sigma_y^2$ and $\sigma_y^1\sigma_x^2$ can be measured without mutual disturbance. However, the product of these two operators can be written as $\sigma_x^1\sigma_y^2 \cdot \sigma_y^1\sigma_x^2 = \sigma_x^1\sigma_y^1 \cdot \sigma_y^2\sigma_x^2 = \sigma_z^1\sigma_z^2$, whose expectation value $\langle\sigma_z^1\sigma_z^2\rangle = -1$. Then it follows from the assumptions I and II that,

$$x_1x_2y_1y_2 = -1, \quad (2.2)$$

which is in contradiction with the Equation 2.1. Soon it was pointed out by Mermin [45] that the contextuality is not a special property of the singlet state, but even holds for single qubit states. The conflict resides in the structure of the theory and is independent of the properties of special states. Though Mermin contextuality is more general in scope, it is interesting to see how the Peres contextuality can be observed experimentally by NMR.

2.3.1 Extension of Peres Contextuality

Peres showed the contextual behavior for a single point by using the operators $\sigma_x^1\sigma_x^1, \sigma_y^1\sigma_y^2$ and $\sigma_z^1\sigma_z^2$. But if we choose two different operators, then we

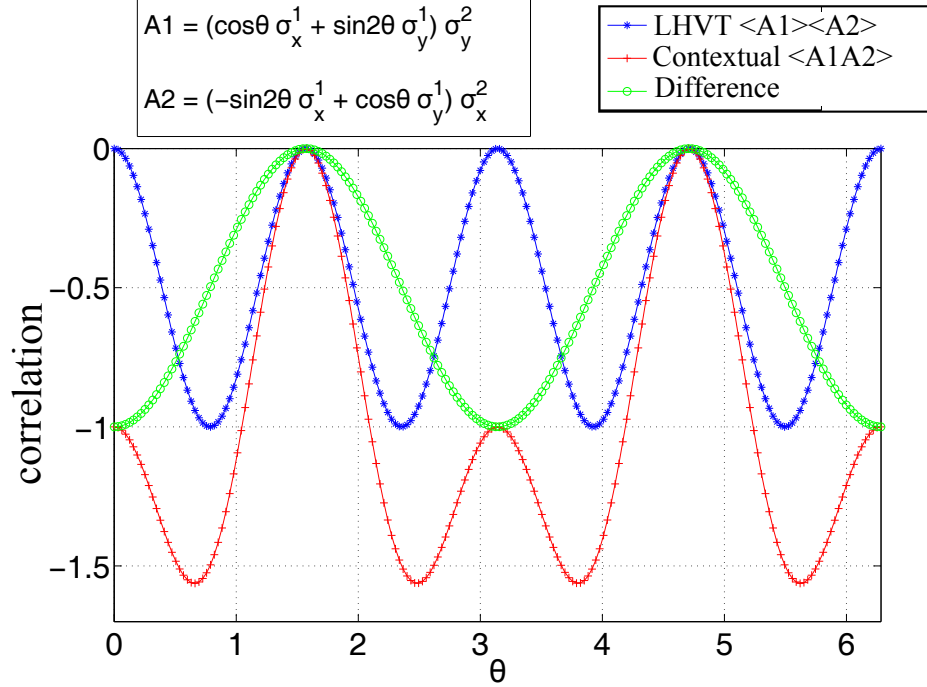


Figure 2.3: The plot for expectation value of quantum mechanics ($\langle A_1 A_2 \rangle$) and local hidden variable theory ($\langle A_1 \rangle \langle A_2 \rangle$) for operators $A1 = (\cos \theta \sigma_x^1 + \sin 2\theta \sigma_y^1) \sigma_y^2$ and $A2 = (-\sin 2\theta \sigma_x^1 + \cos \theta \sigma_y^1) \sigma_x^2$.

can show a continuous violation of local hidden variable theory (LHV). These operators can be $A1 = (\cos \theta \sigma_x^1 + \sin 2\theta \sigma_y^1) \sigma_y^2$ and $A2 = (-\sin 2\theta \sigma_x^1 + \cos \theta \sigma_y^1) \sigma_x^2$. The value of correlation predicted by LHV is different from the value of correlation predicted by contextual theory. The expectation values $\langle A1 \rangle \langle A2 \rangle$, $\langle A1A2 \rangle$ and their difference for the singlet state are shown as a function of θ in Figure 2.3. At values of $\theta = 0$, these operators are same as Peres contextual operators. At $\theta = \pi/2$, the operators are non contextual and there is no difference between $\langle A1 \rangle \langle A2 \rangle$ and $\langle A1A2 \rangle$. At all values of θ , $A(\theta)$ and $B(\theta)$ do commute and can be measured simultaneously. A continuous and periodic transition from contextual to non contextual behavior can be observed. Experimental studies of such a set of operators is helpful in not only understanding contextuality, but also to estimate systematic and random errors in the experiment itself.

2.4 Spin 1 Case

The earlier inequalities were given for spin 1/2 particles in a singlet state. In 2007, Alexander S. Shumovsky *et al.* gave a inequality for spin 1 case[17]. They called it **pentagram inequality**. Although it was state dependent but the number of operators used were only 5 (they were 31 in K-S Theorem.) To derive a Bell type inequality for spin 1 case, we can consider five numbers a_1, a_2, a_3, a_4, a_5 , all take only values $+1$ or -1 . For any values of these operators the following inequality is always followed:

$$a_1a_2 + a_2a_3 + a_3a_4 + a_4a_5 + a_5a_1 \geq -3 \quad (2.3)$$

Let these numbers now be the result of five corresponding two-outcome (± 1) measurements A_1, A_2, A_3, A_4 and A_5 . Then assuming that there exists a joint probability distribution for 2^5 possible measurement outcome combinations, taking the average of inequality 2.3 gives

$$\langle A_1A_2 \rangle + \langle A_2A_3 \rangle + \langle A_3A_4 \rangle + \langle A_4A_5 \rangle + \langle A_5A_1 \rangle \geq -3 \quad (2.4)$$

The operators A_i can be given by $2S_{i_i}^2 - 1$ respectively. These operators can take eigenvalues $a_i = \pm 1$ respectively.

The experimental verification of pentagram inequality is reported for a LASER system [18]. The 3 state spin 1 system (a QUTRIT) is realized by production of single photons distributed in three modes. Three detectors are used to take measurements (decide the mode of photon). Transformations on the initial setup are used to realize all five detectors. Half-wave plates are used to do the transformations. There results show the verification of pentagram inequality.

2.5 Fully Contextual Correlations

Recently Cabello *et al.* has reported that for the graph given in the Figure 2.4, we can construct the following inequality[19]:

$$P(010|012) + P(111|012) + P(01|02) + P(00|03) + P(11|03) + P(00|14) + P(01|25) + P(010|345) + P(111|345) + P(10|35) \geq 3 \quad (2.5)$$

The right hand side of the above inequality is given by the Independence number (the number of pairwise nonlinked vertices) of the graph. Claim: For the given graph that number is 3. In the graph, the number of vertex are 10. Every vertex is connected to 4 vertices. The second vertex, which will be in no contradiction with the chosen vertex, has to be chosen from

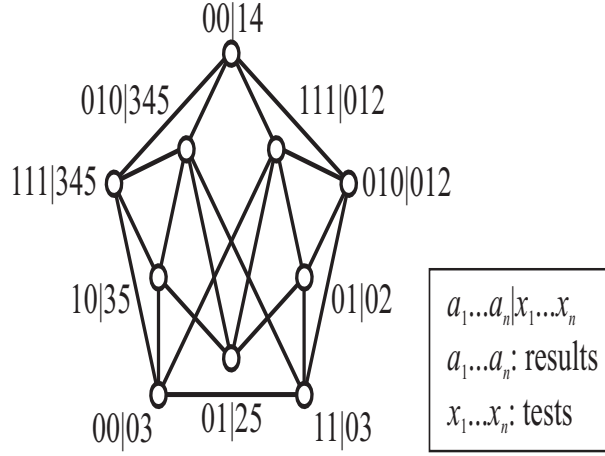


Figure 2.4: Graph showing propositions. Eg. $10|35$ means outcome 1 is obtained when observable 3 is measured, and outcome 0 is obtained when observable 5 is measured. Edges are joining propositions that cannot hold simultaneously. Eg. $00|03$ and $11|03$ are linked, since outcome of measurement 3 is 0 and 1 for the two propositions respectively, which cannot be true at the same time.

the remaining 5 vertices. From these 5 vertices only 2 more vertices can be selected. Thus the claim. The left hand side of the above inequality is found to be equal to 3.5. Calculation of the left hand side can be found in the Appendix A.1. In the above inequality, the operators are:

$$\begin{aligned}
 0 &= \sigma_x \otimes I & 1 &= I \otimes \sigma_z & 2 &= \sigma_x \otimes \sigma_z \\
 3 &= I \otimes \sigma_x & 4 &= \sigma_z \otimes I & 5 &= \sigma_x \otimes \sigma_z
 \end{aligned} \tag{2.6}$$

In the above arrangement of the operators, the operators in row (operators 0,1,2 commutes among themselves, same for operators 3,4,5) and column (operators 0,3 commutes among themselves, same for operators 1,4 and 2,5) commute and they are mutually compatible, hence they can be measured simultaneously. In the probability calculations, only compatible operators are measured. The maximum violation of the inequality is found when two spin system is prepared in state $|\psi\rangle = \frac{1}{\sqrt{2}}(|0\rangle + |3\rangle)$. Here $\langle 0| = (1, 0, 0, 0)$, $\langle 1| = (0, 1, 0, 0)$, $\langle 2| = (0, 0, 1, 0)$, $\langle 3| = (0, 0, 0, 1)$.

Chapter 3

Methods

3.1 NMR Implementation

The NMR Hamiltonian of a weakly coupled 3-qubit system can be written as:

$$\mathcal{H} = - \sum_{i=1}^3 \omega_i I_z^i + 2\pi \sum_{i<j=1}^3 J_{ij} I_z^i I_z^j \quad (3.1)$$

Here ω_i is the larmor frequency of the i^{th} spin, I_z^i is the component in z direction of spin angular momentum of i^{th} spin and J_{ij} is scalar coupling constant between i^{th} and j^{th} spin. The first step of the experiment is to initialize the system in $|000\rangle$ state. The preparation of pure state in a liquid state NMR system at room temperature requires extreme experimental conditions (extremely low temperature or extremely high magnetic field). Hence, one can prepare a "Pseudo-Pure State" (PPS) that mimics a pure state. The equilibrium deviation density matrix for a homonuclear spin system under high temperature and high field approximation is proportional to $I_z^1 + I_z^2 + I_z^3$, where the superscript denotes the qubit number and the subscript denotes the magnetization mode. We have adapted the 'spatial averaging' method proposed by Cory *et al.* [20, 21] for the preparation of $|000\rangle$ PPS state. The NMR pulse sequence for preparing $|000\rangle$ PPS state is shown in Figure 3.1. The 75.52° pulse on qubit 1 and 60° pulse on qubit 2, followed by a crusher gradient creates $\frac{1}{4}I_z^1 + \frac{1}{2}I_z^2 + I_z^3$ state. The rest of the pulse sequence consists of the basic sequence of

$$U[i, j] = [\pi/4]_{\phi}^j \longrightarrow \frac{1}{2J_{ij}} \longrightarrow [\pi/4]_{\phi-90}^j \quad (3.2)$$

with additional π pulses during the free evolution period which refocus the chemical shift evolutions and other J -evolutions, thus making the system

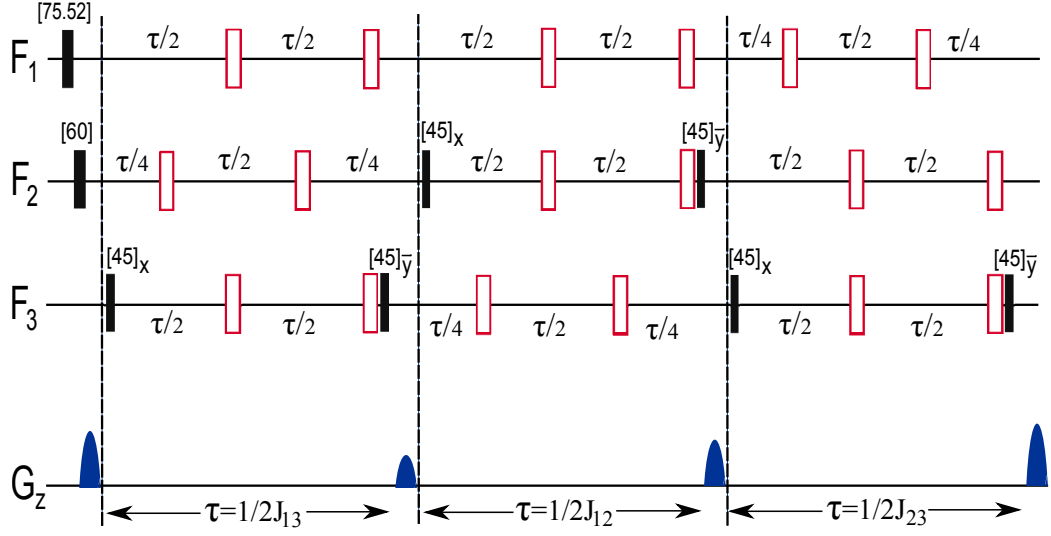


Figure 3.1: Pulse program for the preparation of $|000\rangle$ pseudo pure state. F_1 , F_2 and F_3 represent the three fluorine spins which form the three qubits. The broad and unshaded pulses are π pulses. The flip angle and the phase of the other pulses are mentioned on the top of each of them. Each of the spin selective pulse has been obtained by specially designed strongly modulated pulses having Hilbert-Schmidt fidelity of over 0.99. The pulse program consists of three J evolutions. During the first J evolution period $1/2J_{13}$, the π pulses on F_2 (at $\tau/4$ and $3\tau/4$) refocus J_{23} and J_{12} evolutions, while the π pulses on F_1 and F_3 (at $\tau/2$) retain J_{13} . The additional π pulses on F_1 and F_3 just before the $[\pi/4]_y$ pulse regain the sign of the spin operator terms inverted by the π pulses on F_1 and F_3 in the middle of $1/2J_{13}$ evolution. Similar argument yields the sequence for the J_{12} and J_{23} evolutions.

evolve only under the desired J coupling. Here the superscript j denotes the qubit number and subscript ϕ denotes the phase of the $[\pi/4]$ pulse. G_z is the crusher gradient which removes all the transversal terms and retains only the longitudinal terms. The operator $U[i, j]$ when applied on equilibrium density matrix $I_z^i + I_z^j$ creates $I_z^i + \frac{1}{2}(I_z^i + 2I_z^i I_z^j)$. Therefore, the application of $U[1, 2]$, $U[1, 3]$ and $U[2, 3]$ in the order shown in Figure 3.1 on the density matrix $\frac{1}{4}I_z^1 + \frac{1}{2}I_z^2 + I_z^3$, creates

$$\frac{1}{4} (I_z^1 + I_z^2 + I_z^3 + 2I_z^1 I_z^2 + 2I_z^1 I_z^3 + 2I_z^2 I_z^3 + 4I_z^1 I_z^2 I_z^3) \quad (3.3)$$

which is the spin operator representation of $|000\rangle$ PPS.

3.1.1 Projective Measurement

The next step is to measure the expectation values. Projective measurement has been carried out by the 'clean qubit' method proposed by Moussa *et al.*[15]. To measure the expectation value of an operator A , the method involves applying A on the system controlled by an ancilla qubit (3rd qubit here). The expectation value of the required operator will project on the ancilla qubit and the data can be collected from it. The circuit for the measurement of $\langle \sigma_\phi^1 \sigma_\phi^2 \rangle$ is shown in Figure 3.2. As shown in the Figure 3.2, the final measurement of the ancilla qubit reveals the expectation value of an observable. The state of the ancilla qubit should be one of the eigen state of the observable to be measured. Hence, in our case the measurement of $\langle \sigma_x \rangle$ or $\langle \sigma_y \rangle$ needs $|+\rangle$ state, which can be easily prepared by applying a hadamard gate [23] (a single 90° pulse on the ancilla, which will create the superposition) on state $|0\rangle$ as shown in the Figure 3.2. The detailed mathematical derivation of this protocol can be found here[15].

3.1.2 Density Matrix Tomography

One of the best known method for quantitative measurement of any state is density matrix tomography, which enables us to measure all elements of a general density matrix. However, it is not straightforward to measure them in an NMR system. A 3 qubit general density matrix has all possible terms containing single quantum (SQ), double quantum (DQ), triple quantum (TQ), or zero quantum (ZQ) coherences. But, in NMR, only SQ coherence is directly detectable as signal. Hence, to get the complete knowledge about the whole density matrix, one has to apply suitable pulses which can convert the DQ, TQ and ZQ coherences into the detectable SQ coherence. A set of 6 dif-

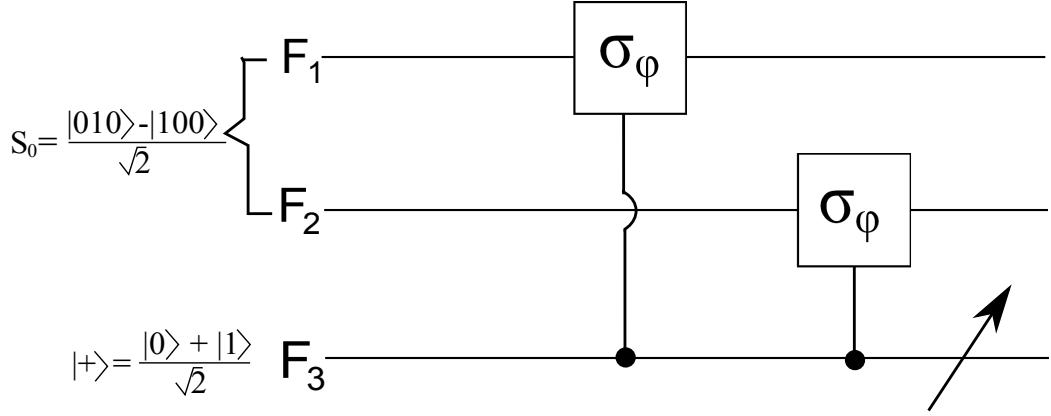


Figure 3.2: Moussa protocol for projective measurement.

ferent experiments are listed below, which are developed for the tomography scheme[22].

1. $\mathbb{1}$
2. $90_y^{1,2,3}$
3. $45_x^{1,2,3}$
4. $d_2 \cdot 180_x^{1,2,3} \cdot d_2 \cdot 90_x^{1,2,3}$
5. $90_x^2 \cdot d_2 \cdot 180_x^{1,2,3} \cdot d_2 \cdot 90_x^3$
6. $90_y^1 \cdot d_2 \cdot 180_x^{1,2,3} \cdot d_2 \cdot 90_y^2$

where $d_2 = 1.075ms$ simulated in such a way that the application of $d_2 \cdot 180_x^{1,2,3} \cdot d_2$ will make all the J couplings as well as chemical shifts refocused during this time. The subscript in the pulse denotes the phase of the pulse and the superscript denotes the qubit number.

3.1.3 Singlet Preparation

Once the PPS is prepared, the next step is to create singlet states between any of the two qubit. The pulse sequence for the singlet states creation is shown in Figure 3.4. PPS state has only longitudinal components and has no transversal components, in terms of density matrix it has only diagonal elements and no off diagonal elements. The initial 90° pulse on qubit 1 and 2 takes the longitudinal components into transverse elements. After that, a suitable J -evolution and application of two 90° pulses makes the

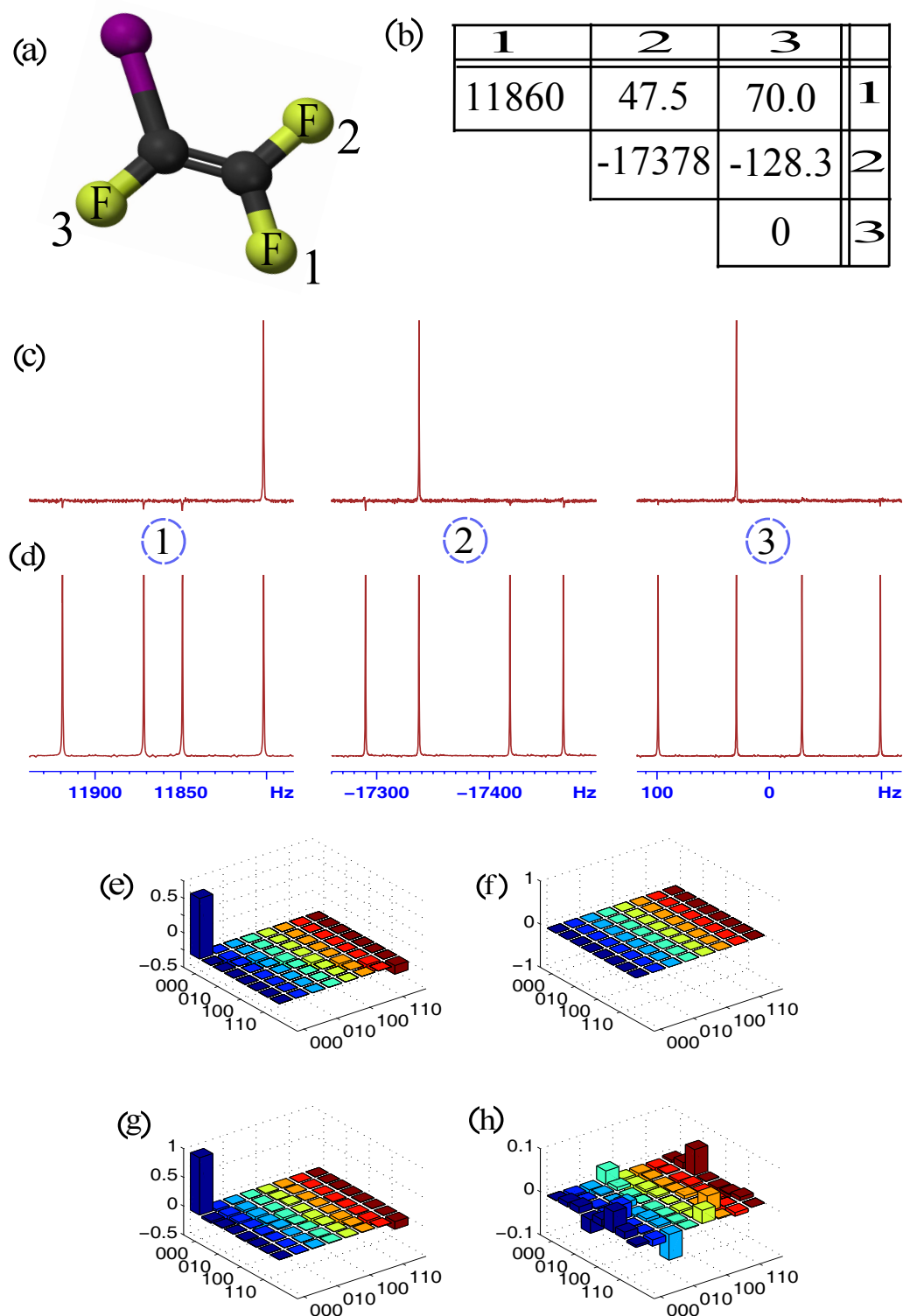


Figure 3.3: The molecular structure in (a) and Hamiltonian parameters in (b) of Iodotrifluoroethylene (C_2F_3I) (5 mg dissolved in 0.5 ml of acetone- d_6), forming a homonuclear three-qubit register. In (b), diagonal and off-diagonal elements correspond to the chemical shifts and the scalar coupling constant, respectively (in Hz). The ^{19}F spectra correspond to the pseudo pure state (c) and the equilibrium mixed state (d). The barplots (e)-(h) correspond to the real (e), (g) and imaginary (f), (h) parts of theoretical (e), (f) and experimental (g), (h) pseudo pure $|000\rangle$ state.

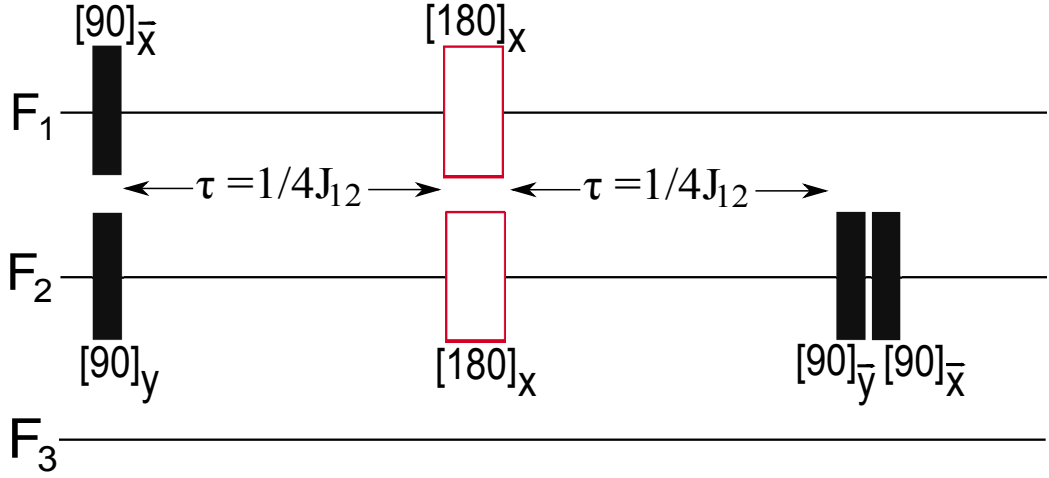


Figure 3.4: Pulse program for the creation of singlet states between F_1 and F_2 spins, starting from $|000\rangle$ pps state. The broad unshaded rectangles denotes π pulses whereas the narrow filled rectangles denotes $\pi/2$ pulses. The phase of the pulses are given at the subscript of particular phase angles. The F_3 spin remains untouched during the whole process.

desired singlet state between qubit 1 and 2. π pulses refocuses couplings with third qubit and also chemical shift during evolution. During this whole period third qubit remains unchanged in $|0\rangle$ state. In terms of spin operator representation, we will have the state $(|010\rangle - |100\rangle)/\sqrt{2}$.

3.2 Experiments

The experimental implementation of the Peres Contextuality has been carried out in a 3-qubit NMR system. The first two qubits are used to prepare singlet states and the third qubit is used as ancilla for measurement outcomes. The system chosen for the experimental implementation is Iodotrifluoroethylene (C2F3I) dissolved in acetone-d6. The experiments have been carried out at 290K in 11.7 Tesla static magnetic field in a Bruker spectrometer using a triple resonance QXI probe. The Fluorine resonance frequency at this field is 470.65 MHz. The three ‘Fluorines’ form the three qubits. The sample specification and equilibrium spectra are given in Figure 3.3. By the application of above described pulse sequence we get $|000\rangle$ PPS state. Spectra corresponding to pseudo pure states are obtained by a linear detection scheme using small flip angle radio frequency pulses. Since the diagonal pseudo pure states have one energy level more populated than all others (having equal distribution), the spectrum should consist ideally of only one transition per

qubit in each case. Quantitative analysis of the pseudo pure states are carried out by density matrix tomography, as described earlier. The purity of the experimentally achieved state ρ with the target PPS state is measured by calculating the correlation:

$$C = \frac{\text{trace}[\rho \cdot \rho_s]}{\sqrt{\text{trace}[\rho^2] \text{trace}[\rho_s^2]}}. \quad (3.4)$$

A high fidelity of 0.982 is obtained with the $|000\rangle$ PPS state. In the next step, singlet state is prepared between spin 1 and spin 2 by applying the pulse sequence described above. As singlet state is a ZQ coherence, it has no readily detectable signal output. However, it can be indirectly detected by applying a delay $\frac{1}{4\Delta\nu}$ ($\Delta\nu$ = chem. shift between spin 1 & 2) and a 90° pulse on spin 1 & 2. The anti phase magnetization of singlet states is shown in Figure 3.5. The ancilla qubit (spin 3) get untouched and hence no signal is detected at this point. The density matrix tomography of this state gives fidelity of 0.966.

The evolution of the ancilla qubit during the whole procedure is shown in Figure 4.1. At equilibrium spectra, all four possible transitions are there and show all 4 lines. PPS state shows only 1 line, as expected, due to only one possible transition for this spin. After applying a Hadamard gate on PPS state, it has two possible transitions. Now this set the perfect platform to do the controlled operation on spins and be detected by the ancilla qubit. The CNOT gates (flips one spin conditional on the state of the other)[23] are implemented using strongly modulated radio frequency pulses of duration approximately 10ms. These gates are robust against radio frequency and magnetic field inhomogeneity.

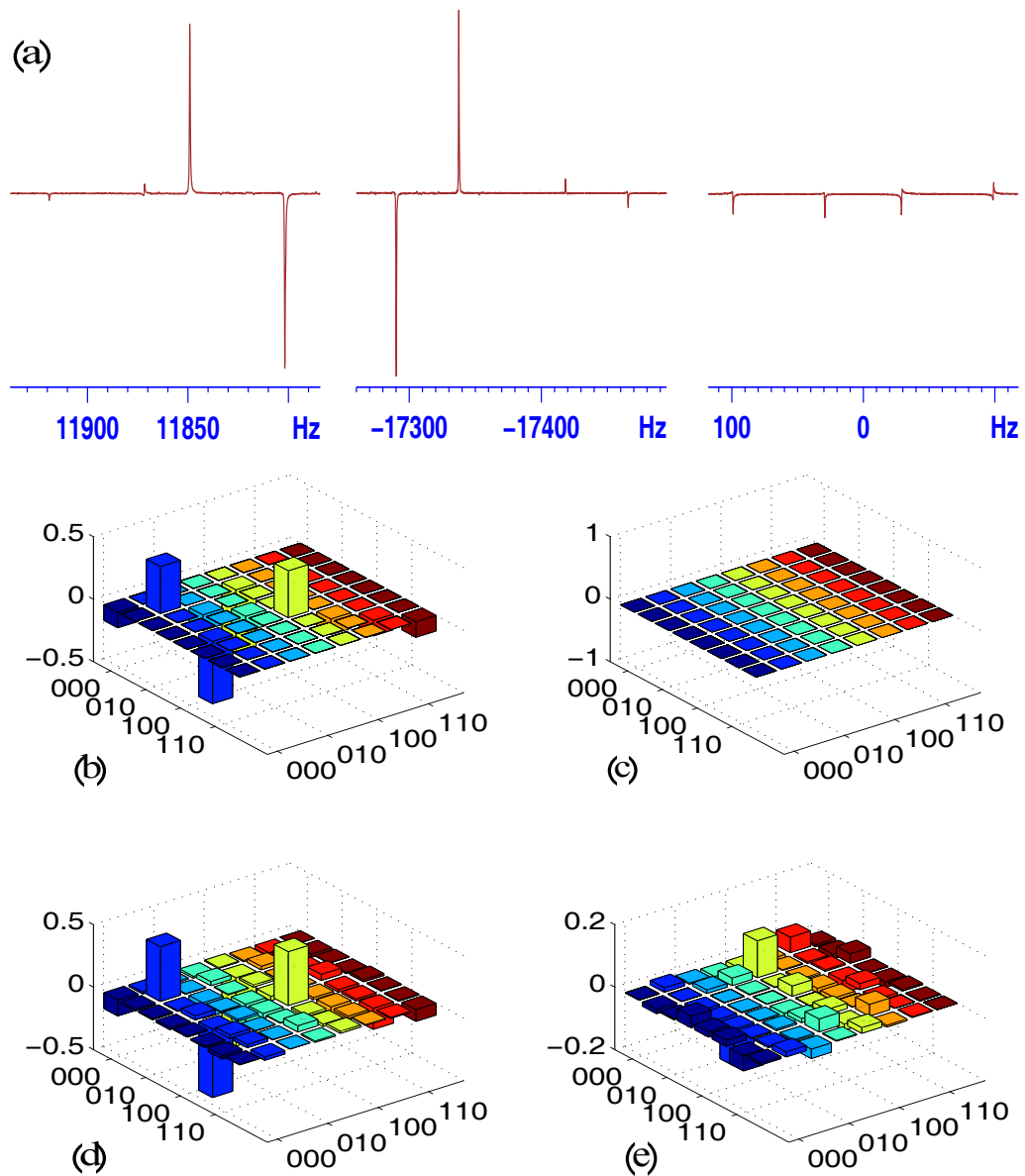


Figure 3.5: (a) The anti phase singlet state spectra derived by applying a detection pulse on spin 1 & 2. The barplots (b) and (c) are the real and imaginary parts of theoretical values respectively and the barplots (d) and (e) are the real and imaginary parts of experimental values respectively for density matrix of $(|010\rangle - |100\rangle)/\sqrt{2}$ state.

Chapter 4

Results

We are reporting the first successful experimental demonstration of Peres contextuality through NMR.

4.1 Continuous Operator for Demonstration of Contextuality

We have found a new set of operators which shows a continuous difference in the expectation values of local hidden variable theory and quantum mechanics.

4.2 Preparation of High Quality Singlet State

Preparation of pure state in NMR system demands extreme experimental conditions (extremely low temperature and extremely high magnetic field). However, one can avoid preparing a pure state by preparing a pseudo pure state (PPS), which mimics the pure state. On the course of preparing high fidelity singlet state, it is necessary to prepare a PPS state. Even for the PPS, the purity factor is 10^{-5} . Although the purity factor is very less, we are able to prepare a good fidelity singlet state. The fidelity of our singlet state is 0.966 (which is the traceless part of the density matrix). We have used Moussa protocol on this singlet state to demonstrate Peres contextuality.

4.3 Obtaining Contextual Expectation Values

The spectra of the ancilla qubit after applying CNOT gates are shown in Figure 4.1. The expectation values of the specified operators are simply the

area under the curve. Comparing with the reference spectra (which has value 1), we get fairly good agreement with the theoretical prediction. The expectation values for the operators $\langle \sigma_x^1 \sigma_y^2 \rangle$ and $\langle \sigma_y^1 \sigma_x^2 \rangle$ are nearly 0 as expected (dispersive spectra) Figure 4.1(f), (g). Again the expectation values for the operator $\langle \sigma_x^1 \sigma_x^2 \rangle$ and $\langle \sigma_y^1 \sigma_y^2 \rangle$ are nearly -1 , whereas the expectation value for $\langle \sigma_x^1 \sigma_y^2 \sigma_y^1 \sigma_x^2 \rangle$ Figure 4.1(d), (e), (h) is also -1 .

Experimentally achieved results are well matched with the theoretically expected values (as shown in Table 4.1) and thus proves the contextual nature of quantum theory.

	Theory	Experiment
$\sigma_x^1 \sigma_x^2$	-1	-0.89
$\sigma_y^1 \sigma_y^2$	-1	-0.89
$\sigma_x^1 \sigma_y^2 \sigma_y^1 \sigma_x^2$	-1	-0.90

Table 4.1: Results

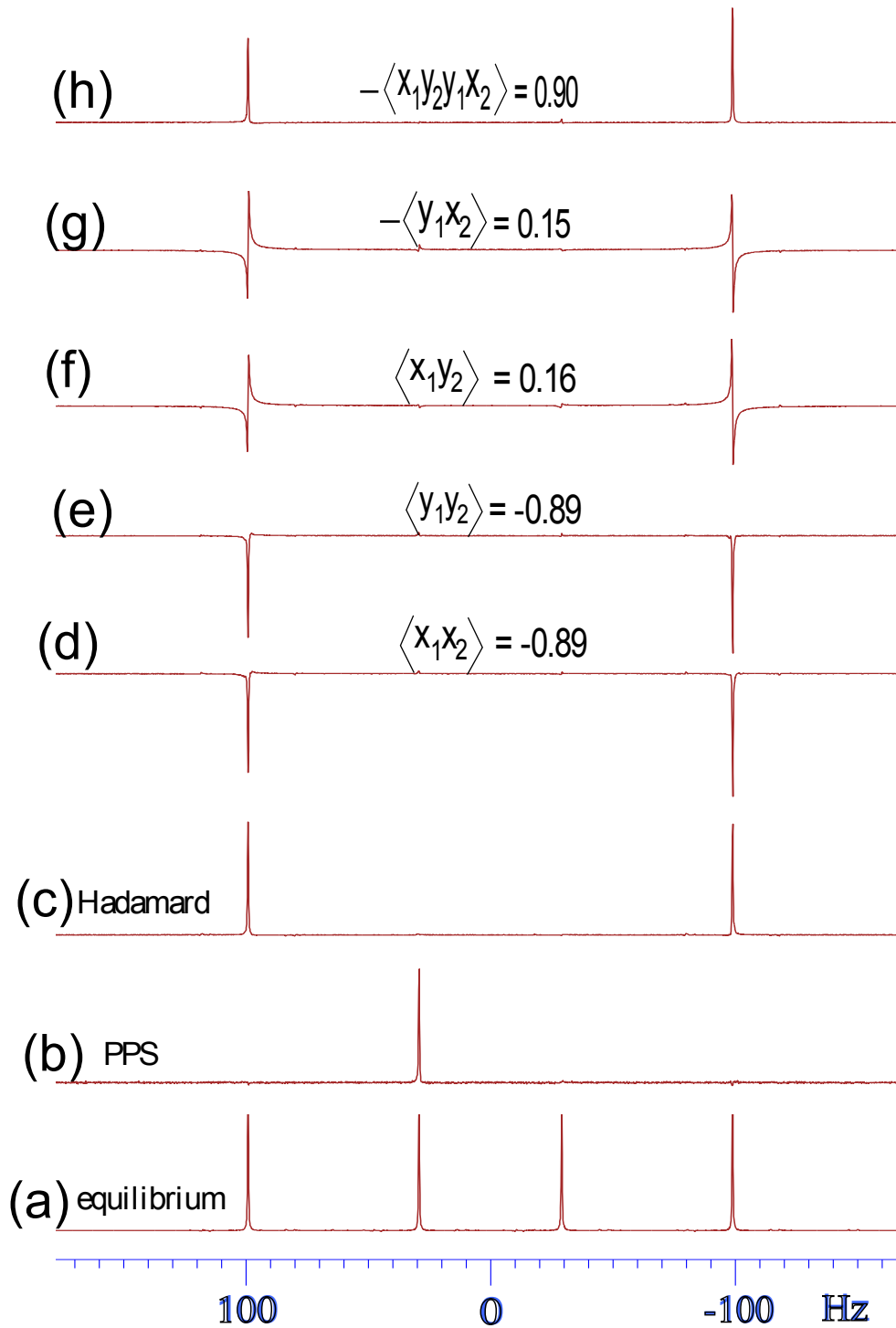


Figure 4.1: The spectra of ancilla qubit during various time instant of the experimental evolution. (a) Equilibrium spectra, (b) PPS spectra achieved by applying a small angle detection pulse, (c) spectra achieved after applying the Hadamard gate on ancilla qubit. (d)-(h) showing spectra of the ancilla qubit after doing (d) $\langle X_1 X_2 \rangle$, (e) $\langle Y_1 Y_2 \rangle$, (f) $\langle X_1 Y_2 \rangle$, (g) $\langle Y_1 X_2 \rangle$, (h) $\langle X_1 Y_2 Y_1 X_2 \rangle$ measurement on spin '1/2' singlet. The numerical results of the expectation values of the corresponding measurements written on the spectra.

Chapter 5

Discussion

We have reported the first experimental demonstration of Peres contextuality using NMR. We used three spin-1/2 nuclei (^{19}F) of Iodotrifluoroethylene and prepared two of them in a pseudo singlet state and used the third spin as ancilla. Using Moussa protocol, we could measure the expectation values of different contextual operators. The results are summarized in the Table 5.1. The systematic errors between the theory and experiment are due to gate

	LHVT	Quantum Theory	Experiment
$\sigma_x^1 \sigma_x^2$	-1	-1	-0.89
$\sigma_y^1 \sigma_y^2$	-1	-1	-0.89
$\sigma_x^1 \sigma_y^2 \sigma_y^1 \sigma_x^2$	+1	-1	-0.90

Table 5.1: results

imperfection and decoherence. The random errors are much smaller than these systematic errors. Apart from these errors, there appears a general agreement between quantum theory and NMR experiments.

Local hidden variable theories have attempted to render quantum mechanics "complete" by arguing pre-measurement eigenvalues to quantum states. Our experimental verification of Peres contextuality demonstrates that such an assignment is not possible and indicates the intrinsic contextual nature of quantum systems.

References

- [1] A. Einstein, B. Podolsky, and N. Rosen, Can Quantum-Mechanical Description of Physical Reality be Considered Complete, *Physical Review* (1935), **47**, 777-780.
- [2] Asher Peres, Incompatible Results of Quantum Measurements, *Physics Letters A* (1990), **151**, 107-108.
- [3] John S. Bell, On the Einstein Podolsky Rosen Paradox, *Physics* (1964), **1**, 195-200.
- [4] S. Kochen and E.P. Specker, The problem of Hidden Variables in Quantum Mechanics, *Journal of Mathematics and Mechanics* (1967), **17**, 59-87.
- [5] John S. Bell, On the Problem of Hidden Variables in Quantum Mechanics (1966), *Reviews of Modern Physics*, **38**, 447-452.
- [6] Adán Cabello, Simple Unified Proof of State-Independent Contextuality, [arXiv:1112.5149v1](https://arxiv.org/abs/1112.5149v1).
- [7] Elias Amselem, Magnus Rådmark, Mohamed Bourennane, and Adán Cabello, State-Independent Quantum Contextuality with Single Photons, *Physical Review Letters* (2009), **103**, 160405.
- [8] B. H. Liu, Y. F. Huang, Y. X. Gong, F. W. Sun, Y. S. Zhang, C. F. Li, and G. C. Guo, Experimental Demonstration of Quantum Contextuality with Non entangled Photons, *Physical Review A* (2009), **80**, 044101.
- [9] G. Kirchmair, F. Zähringer, R. Gerritsma, M. Kleinmann, O. Gühne, A. Cabello, R. Blatt and C. F. Roos, State-Independent Experimental Test of Quantum Contextuality, *Nature*(2009), **460**, 494-498.
- [10] Adán Cabello, Stefan Filipp, Helmut Rauch, and Yuji Hasegawa, Proposed Experiment for Testing Quantum Contextuality with Neutrons, *Physical Review Letters* (2008), **100**, 130404.

- [11] H. Bartosik, J. Klepp, C. Schmitzer, S. Sponar, A. Cabello, H. Rauch, and Y. Hasegawa, Experimental Test of Quantum Contextuality in Neutron Interferometry, *Physical Review Letters* (2009), **103**, 040403.
- [12] Sixia Yu and C.H. Oh, State-Independent Proof of Kochen-Specker Theorem with 13 Rays, arXiv:1109.4396v1.
- [13] N. David Mermin, Hidden Variables and the Two Theorems of John Bell, *Physical Review Letters* (1993), **65**, 803-815.
- [14] N. David Mermin Simple Unified Form for the Major No-hidden-variables Theorems, *Physical Review Letters* (1990), **65**, 3373-3376.
- [15] Osama Moussa, Colm A. Ryan, David G. Cory and Raymond Laflamme, Testing Contextuality on Quantum Ensembles with One Clean Qubit, *Physical Review Letters* (2010), **104**, 160501.
- [16] Asher Peres, *Quantum Theory: Concepts and Methods*, Kluwer Academic Publishers, New York (2002).
- [17] Alexander A. Klyachko, M. Ali Can, Sinem Binicioglu and Alexander S. Shumovsky, Simple Test for Hidden Variables in Spin-1 Systems, *Physical Review Letters* (2008), **101**, 020403.
- [18] Radek Lapkiewicz, Peizhe Li, Christoph Schaeff, Nathan K. Langford, Sven Ramelow, Marcin Wiesniak and Anton Zeilinger, Experimental Non-classicality of an Indivisible Quantum System, *Nature* (2011), **474**, 490-493.
- [19] Elias Amsalem, Lars Eirik Danielsen, Antonio J. López-Tarrida, Josté R. Portillo, Mohamed Bourennane, and Adan Cabello, Experimental Fully Contextual Correlations, arXiv:1111.3743v1.
- [20] David G. Cory, Amr F. Fahmy and Timothy F. Havel, Ensemble Quantum Computing by NMR Spectroscopy, *Proc. Natl. Acad. Sci. USA* (1997), **94**, 1634-1639.
- [21] Avik Mitra, T. S. Mahesh, and Anil Kumar, NMR Implementation of Adiabatic SAT Algorithm using Strongly Modulated Pulses, *J. Chem. Phys.* (2008), **128**, 124110.
- [22] S. S. Roy and T. S. Mahesh, Density Matrix Tomography of Singlet States, *J. Magn. Reson.* 2010, **206**, 127.

- [23] Michael A. Nielsen and Isaac L. Chuang, Quantum Computation and Quantum Information, Cambridge University Press, Cambridge (2000).

Appendix A

Long Proofs

A.1 Calculation of Left Hand Side of Equation 2.5

The state for the measurements is $|\psi\rangle = \frac{1}{\sqrt{2}}(|0\rangle + |3\rangle)$. Where $\langle 0| = (1, 0, 0, 0)$, $\langle 3| = (0, 0, 0, 1)$. $P(010|012)$ is the probability of getting results of our measurement as 0,1,0 when operators 0,1,2 are measured respectively. To calculate the probability we have to find the overlap of the given state with the eigenvector of the operator. As here more than one operators are involved, we should calculate the overlap of the state with the common eigenvector of the operators in the expression.

Now to calculate the probability $P(010|012)$, we should take simultaneously the condition for eigenvalue 0 for operator $\sigma_x \otimes I$, eigenvalue 1 for operator $I \otimes \sigma_z$ and eigenvalue 0 for operator $\sigma_x \otimes \sigma_z$. Taking the required

conditions from the Table A.1, for general eigenvector $\begin{pmatrix} x_1 \\ x_2 \\ x_3 \\ x_4 \end{pmatrix}$, we get the

normalized eigenvector ω_1 as $\frac{1}{\sqrt{2}} \begin{pmatrix} 1 \\ 0 \\ -1 \\ 0 \end{pmatrix}$ or $\frac{1}{\sqrt{2}} \begin{pmatrix} -1 \\ 0 \\ 1 \\ 0 \end{pmatrix}$. Calculating the

probability, to find the overlap of the given state with the eigenvector, by the formula $\langle \psi | \omega_1 \omega_1^\dagger | \psi \rangle$, we get probability $P(010|012) = 0.25$ for both eigenvectors (this is the case for all the propositions).

Similarly, normalized eigenvectors and the probability corresponding to the given propositions of operators are shown in the Table A.2.

Operator number	Operator	eigenvalue 0	eigenvalue 1
0	$\sigma_x \otimes I$	$x_3 = -x_1$ $x_4 = -x_2$ $x_1 = -x_3$ $x_2 = -x_4$	$x_3 = x_1$ $x_4 = x_2$ $x_1 = x_3$ $x_2 = x_4$
1	$I \otimes \sigma_z$	$x_1 = -x_1$ $-x_2 = -x_2$ $x_3 = -x_3$ $-x_4 = -x_4$	$x_1 = x_1$ $-x_2 = x_2$ $x_3 = -x_3$ $-x_4 = x_4$
2	$\sigma_x \otimes \sigma_z$	$x_3 = -x_1$ $-x_4 = -x_2$ $x_1 = -x_3$ $-x_2 = -x_4$	$x_3 = x_1$ $-x_4 = x_2$ $x_1 = x_3$ $-x_2 = x_4$
3	$I \otimes \sigma_x$	$x_2 = -x_1$ $x_1 = -x_2$ $x_4 = -x_3$ $x_3 = -x_4$	$x_1 = x_2$ $x_4 = x_2$ $x_4 = x_3$ $x_3 = x_4$
4	$\sigma_z \otimes I$	$x_1 = -x_1$ $x_2 = -x_2$ $-x_3 = -x_3$ $-x_4 = -x_4$	$x_1 = x_1$ $x_2 = x_2$ $-x_3 = x_3$ $-x_4 = x_4$
5	$\sigma_z \otimes \sigma_x$	$x_2 = -x_1$ $x_1 = -x_2$ $-x_4 = -x_3$ $-x_3 = -x_4$	$x_2 = x_1$ $x_1 = x_2$ $-x_4 = x_3$ $-x_3 = x_4$

Table A.1: Conditions for the eigenvectors of the operators

Condition	eigenvector	Probability ($\langle \psi \omega_1 \omega_1^\dagger \psi \rangle$)
P(010 012)	$\frac{1}{\sqrt{2}} \begin{pmatrix} 1 \\ 0 \\ -1 \\ 0 \end{pmatrix}$ or $\frac{1}{\sqrt{2}} \begin{pmatrix} -1 \\ 0 \\ 1 \\ 0 \end{pmatrix}$	0.25
P(111 012)	$\frac{1}{\sqrt{2}} \begin{pmatrix} 1 \\ 0 \\ 1 \\ 0 \end{pmatrix}$ or $\frac{1}{\sqrt{2}} \begin{pmatrix} -1 \\ 0 \\ -1 \\ 0 \end{pmatrix}$	0.25
P(01 02)	$\frac{1}{\sqrt{2}} \begin{pmatrix} 0 \\ 1 \\ 0 \\ -1 \end{pmatrix}$ or $\frac{1}{\sqrt{2}} \begin{pmatrix} 0 \\ -1 \\ 0 \\ 1 \end{pmatrix}$	0.25
P(00 03)	$\frac{1}{2} \begin{pmatrix} -1 \\ 1 \\ 1 \\ -1 \end{pmatrix}$ or $\frac{1}{2} \begin{pmatrix} -1 \\ 1 \\ 1 \\ -1 \end{pmatrix}$	0.5
P(11 03)	$\frac{1}{2} \begin{pmatrix} 1 \\ 1 \\ 1 \\ 1 \end{pmatrix}$ or $\frac{1}{2} \begin{pmatrix} -1 \\ -1 \\ -1 \\ -1 \end{pmatrix}$	0.5
P(00 14)	$\begin{pmatrix} 0 \\ 0 \\ 0 \\ 1 \end{pmatrix}$ or $\begin{pmatrix} 0 \\ 0 \\ 0 \\ -1 \end{pmatrix}$	0.5
P(01 25)	$\frac{1}{2} \begin{pmatrix} 1 \\ 1 \\ -1 \\ 1 \end{pmatrix}$ or $\frac{1}{2} \begin{pmatrix} -1 \\ -1 \\ 1 \\ -1 \end{pmatrix}$	0.5
P(010 345)	$\frac{1}{\sqrt{2}} \begin{pmatrix} 1 \\ -1 \\ 0 \\ 0 \end{pmatrix}$ or $\frac{1}{\sqrt{2}} \begin{pmatrix} -1 \\ 1 \\ 0 \\ 0 \end{pmatrix}$	0.25
P(111 345)	$\frac{1}{\sqrt{2}} \begin{pmatrix} 1 \\ 1 \\ 0 \\ 0 \end{pmatrix}$ or $\frac{1}{\sqrt{2}} \begin{pmatrix} -1 \\ -1 \\ 0 \\ 0 \end{pmatrix}$	0.25
P(10 35)	$\frac{1}{\sqrt{2}} \begin{pmatrix} 0 \\ 0 \\ 1 \\ 1 \end{pmatrix}$ or $\frac{1}{\sqrt{2}} \begin{pmatrix} -0 \\ 0 \\ -1 \\ -1 \end{pmatrix}$	0.25

Table A.2: Probability for the given propositions of operators